A SHORT NOTE ON ANTIMONOTONICITY IN BIFURCATION DIAGRAMS OF FAMILIES OF ONE-DIMENSIONAL MAPS

TORE M. JONASSEN

ABSTRACT. We present an example of a one-parameter family of one-dimensional maps with both ways pitch-forks in its bifurcation diagram. Then we discuss non-monotone families, and give arguments why existence antimonotone parameter values are expected to be generic in one-dimensional one-parameter families bifurcating from a periodic attractor to a chaotic invariant set.

1. INTRODUCTION

In [K&K&Y] it is proven that both ways pitch-fork bifurcations occur near any non-degenerate homoclinic tangency in one-parameter family of dissipative plane C^3–diffeomorphisms. For one-dimensional maps the situation is different. It can be proven that the logistic family $x \mapsto \alpha - x^2$ has only pitch-forks directed one way. The logistic family is belived to be exceptional in this respect among smooth one-dimensional maps. Here we discuss a simple one-parameter family with both ways pitch-fork bifurcations in its bifurcation diagram, and explain why we should expect such behavior. We then show that the family has a simple period-two attractor for all α larger than some α_p. The complement of the domain of attraction of this period two orbit consists of a expansive chaotic Cantor-set. In particular this chaotic set contains non-degenerate homoclinic orbits. The β-lift of f_α (see [J]), $F_{\beta,\alpha}(x,y) = (f_\alpha(x) + \beta y, x)$, is an interesting family of plane diffeomorphisms since $F_{\beta,\alpha}$ does not increase norm, and $F^2_{\beta,\alpha}$ contracts norm, outside some compact set $C(\alpha,\beta)$ for $0 < |\beta| < 1$. Hence no orbits escape this compact.

We then show how to obtain non-monotone families from simple cubic systems, and use this construction to obtain infinite cascades of both-ways pitch-forks. We then argue heurictically that the existence of anti-monotone parameter values in one-dimensional one-parameter multi-modal systems is a generic property, and support this by numerical evidence. It is not known if anti-monotone parameter values exist in all generic bi-modal families with a chaotic attractor, but this is among the anti-monotone specialists believed to be the case [K].

As a general reference for one-dimensional systems we have used [Pres].

2. THE EXAMPLE

Let $\tilde{f}_\alpha : \mathbb{R} \longrightarrow \mathbb{R}$ be defined by

$$\tilde{f}_\alpha(x) = -\alpha \cos(3x) \exp\left(-\frac{x^2}{10}\right)$$

for $\alpha > 0$. We note that $\tilde{f}_\alpha(\mathbb{R}) = I_\alpha$ is a compact set given by $I_\alpha = [-\alpha, k\alpha]$ where $k = -\tilde{f}_\alpha(\nu_1)$ with $\nu_1 = \min\{\nu : \tilde{f}'_\alpha(\nu) = 0, \nu > 0\}$. Hence we may consider the system

$$f_\alpha : I_\alpha \longrightarrow I_\alpha$$

where $f_\alpha = \tilde{f}_\alpha|_{I_\alpha}$.

f_α is easily seen to be a piecewise monotone mapping of I_α, and there is a well-defined mapping

$$\tau : \mathbb{R}^+ \longrightarrow \mathbb{N} : \alpha \mapsto n$$

Key words and phrases. bifurcation, chaos, numerical experiment.

counting the number of turning points of f_α. We see that τ has a countable number of discontinuities given by

$$0 = \alpha_0 < \alpha_1 < \alpha_2 < \cdots < \alpha_n < \dots$$

and that $\tau(\alpha) = n$ if $\alpha \in (\alpha_{n-1}, \alpha_n)$. It is shown by an easy calculation that $\alpha_1 \approx 1.02447$, $\alpha_2 \approx 1.14048$, $\alpha_3 \approx 2.04914$ and $\alpha_4 \approx 2.2812$. Hence the family is unimodal in the parameter-range $(0, \alpha_1)$, bi-modal in (α_1, α_2) and tri-modal in (α_2, α_3). Several graphs of f_α, f_α^2 and f_α^3 are shown in the illustration below.

We note that $f_\alpha(x) = f_\alpha(-x)$. Furthermore $f_\alpha(I_\alpha) \subset I_\alpha$ where the inclution is strict if $\alpha \in (0, \alpha_1)$, and $f_\alpha(I_\alpha) = I_\alpha$ if $\alpha > \alpha_1$.

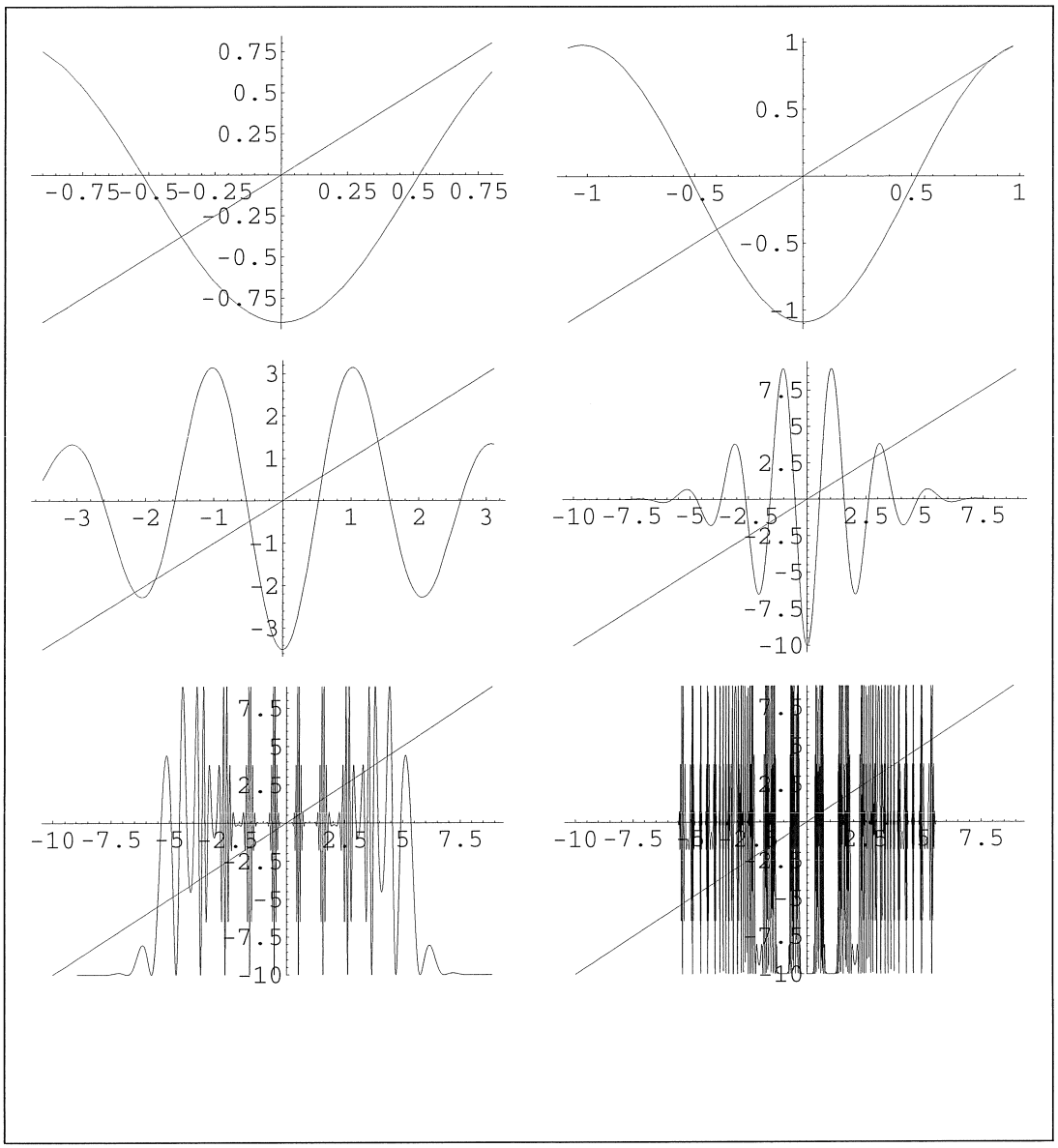

Top left: The graph of f_α in the unimodal parameter range with $\alpha = 0.9$. **Top right:** The graph of f_α in the bimodal parameter range with $\alpha = 1.09$. **Middle left:** The graph of f_α in the multimodal parameter range with $\alpha = 3.5$. **Middle right:** The graph of f_α with $\alpha = 10$ **Bottom left:** The graph of f_α^2 with $\alpha = 10$ **Bottom right:** The graph of f_α^3 with $\alpha = 10$. The function f_α^3 is clearly oscillating.

3. Both-ways pitchforks in the bimodal parameter range

For $\alpha > \alpha_1 \approx 1.02447$ with $\alpha < \alpha_2$ the family is bi-modal. We will in this section explain why we should expect to see non-monotone behaviour in the bifurcation diagram of the family $\{f_\alpha\}$ in the bi-modal parameter range.

Let $c_1 < c_2 = 0$ denote the two critical points of f_α. Clearly c_1 and c_2 are independent of α. We also note that the zeroes of f_α are independent of α. The zeros are preimages of c_2. For α close to α_1 there are two zeros, z_1 and z_2. Hence we divide the interval $I = [l, r]$ with α-independent points as follows:

$$l(\alpha) < c_1 < z_1 < c_2 < z_2 < r(\alpha)$$

We note that f_α is increasing in $[l, c_1]$ and $[c_2, r]$, and decreasing in $[c_1, c_2]$. Furthermore we have $f_\alpha(z_i) = c_2$, $f_\alpha(c_1) = r$, l close to c_1 and $f_\alpha(x) < x$ if $x \in [c_2, r]$, if α close to α_1.

Assume that f_α has periodic orbits of the following type:

$$x_1 \xrightarrow{f_\alpha} x_2 \xrightarrow{f_\alpha} x_3 \xrightarrow{f_\alpha} \cdots \xrightarrow{f_\alpha} x_{n-1} \xrightarrow{f_\alpha} x_n \xrightarrow{f_\alpha} x_{n+1} = x_1$$

where $x_1 \in (l, c_1)$, $x_2 > x_3 > \cdots > x_{n-1}$ where x_{n-1} is close to z_2 and x_n is close to c_2. It can be shown that such stable periodic orbits exist.

Assume that this orbit undergoes a period-doubling bifurcation and becomes unstable at $\alpha = \alpha'$. Then

$$f^n_{\alpha'}(x_i) = x_i \quad \text{with} \quad \frac{\partial f^n_{\alpha'}}{\partial x}(x_i) = -1.$$

From the above we see that $x_1 \in (l, c_1)$, $x_2, \ldots, x_{n-2} \in (z_2, r)$, $x_{n-1} \in (c_2, z_2)$ and $x_n \in (z_1, c_2)$ since the derivative

$$\frac{\partial f^n_{\alpha'}}{\partial x}(x_i) = \prod_{k=1}^{n} \frac{\partial f_{\alpha'}}{\partial x}(x_k) = -1$$

is negative. Hence $\frac{\partial f^n_\alpha}{\partial x}(x_i(\alpha)) < -1$ in some interval $(\alpha', \alpha' + \epsilon)$ for some $\epsilon > 0$ by the assumption that the periodic orbit undergoes a period-doubling bifurcation, and becomes unstable.

Consider the periodic point $x_{n-1}(\alpha)$. We will show that $\frac{\partial x_{n-1}}{\partial \alpha} > 0$. Consider the equation

$$f^n(x(\alpha), \alpha) = x(\alpha).$$

By the chain rule we find

$$\frac{\partial x}{\partial \alpha} = \frac{\frac{\partial f^n}{\partial \alpha}(x(\alpha), \alpha)}{1 - \frac{\partial f^n}{\partial x}(x(\alpha), \alpha)}$$

By assumption we have $\frac{\partial f^n}{\partial x}(x(\alpha), \alpha) < -1$, so the sign of $\frac{\partial x}{\partial \alpha}$ equals the sign of $\frac{\partial f^n}{\partial \alpha}(x(\alpha), \alpha)$. Let $p = x_{n-1}$. Then $f(p, \alpha) = x_n$, $f^2(p, \alpha) = x_1$ and $f^3(p, \alpha) = x_2$. Now since $\frac{\partial f_\alpha}{\partial x}$ is negative in (c_1, c_2), non-negative else, and $\frac{\partial f}{\partial \alpha}$ is negative in (z_1, z_2), non-negative else, we see from the assumption of the location of the periodic orbit that

$$\frac{\partial f_\alpha}{\partial \alpha}(p) < 0, \quad \frac{\partial f_\alpha}{\partial \alpha}(f(p)) < 0, \quad \frac{\partial f_\alpha}{\partial x}(f(p)) < 0$$

and that the derivatives at all other points on the orbit are positive. From the chain rule we obtain the following set of recursive equations for $\frac{\partial f^n}{\partial \alpha}(x(\alpha), \alpha)$:

$$\begin{aligned}
\frac{\partial f^n_\alpha}{\partial \alpha}(p) &= \frac{\partial f_\alpha}{\partial x}(f^{n-1}_\alpha(p)) \frac{\partial f^{n-1}_\alpha}{\partial \alpha}(p) + \frac{\partial f_\alpha}{\partial \alpha}(f^{n-1}(p)) \\
\frac{\partial f^{n-1}_\alpha}{\partial \alpha}(p) &= \frac{\partial f_\alpha}{\partial x}(f^{n-2}_\alpha(p)) \frac{\partial f^{n-2}_\alpha}{\partial \alpha}(p) + \frac{\partial f_\alpha}{\partial \alpha}(f^{n-2}_\alpha(p)) \\
&\vdots \\
\frac{\partial f^3_\alpha}{\partial \alpha}(p) &= \frac{\partial f_\alpha}{\partial x}(f^2_\alpha(p)) \frac{\partial f^2_\alpha}{\partial \alpha}(p) + \frac{\partial f_\alpha}{\partial \alpha}(f^2_\alpha(p)) \\
\frac{\partial f^2_\alpha}{\partial \alpha}(p) &= \frac{\partial f_\alpha}{\partial x}(f_\alpha(p)) \frac{\partial f_\alpha}{\partial \alpha}(p) + \frac{\partial f_\alpha}{\partial \alpha}(f_\alpha(p))
\end{aligned}$$

We find that

$$\frac{\partial f_\alpha^2}{\partial \alpha}(p) = \frac{\partial f_\alpha}{\partial x}(f_\alpha(p))\frac{\partial f_\alpha}{\partial \alpha}(p) + \frac{\partial f_\alpha}{\partial \alpha}(f_\alpha(p)) > -1$$

and since $f_\alpha^2(p)$ is close to c_1 we have $\frac{\partial f_\alpha}{\partial x}(f_\alpha^2(p))$ close to zero. Hence

$$\frac{\partial f_\alpha^3}{\partial \alpha}(p) = \frac{\partial f_\alpha}{\partial x}(f_\alpha^2(p))\frac{\partial f_\alpha^2}{\partial \alpha}(p) + \frac{\partial f_\alpha}{\partial \alpha}(f_\alpha^2(p)) > \frac{\partial f_\alpha}{\partial \alpha}(f_\alpha^2(p)) - \frac{\partial f_\alpha}{\partial x}(f_\alpha^2(p)) \approx k - \epsilon > 0$$

where k is given in section 2, and $\epsilon > 0$ is a small number. By finite induction we see that $\frac{\partial f^n}{\partial \alpha}(p(\alpha), \alpha) > 0$. We conclude that $\frac{\partial x_{n-1}}{\partial \alpha} > 0$, so we should expect that $x_{n-1}(\alpha'') = z_2$ for some $\alpha'' > \alpha'$. In particular we have $\frac{\partial f_{\alpha^*}^n}{\partial x}(x_i) = -1$ for some α^* with $\alpha' < \alpha^* < \alpha''$. Hence we should observe both-ways pitchforks assosiated with such periodic orbits. Numerical experiments show that this is indeed the cases. Figures 1 – 6 show infinite cascades of pitch-forks directed both-ways in the indicated parameter range.

4. The family has a period-two attractor when α is large

We will show that f_α has a period-two attractor for all $\alpha > \alpha_p$ for some $\alpha_p > 0$. We also compute an upper bound for α_p. In the following let $J = [-\pi/12, \pi/12]$.

Lemma 1. *If $x \in J$ then $f_\alpha(x) < -\alpha/2$.*

Proof. If $x \in J$ then $\cos(3x) \geq \frac{1}{2}\sqrt{2}$ and if $x \in [-\sqrt{5\ln 2}, \sqrt{5\ln 2}]$ then $\exp(-x^2/10) \geq \frac{1}{2}\sqrt{2}$. Clearly $J \subset (-\sqrt{5\ln 2}, \sqrt{5\ln 2})$ so

$$f_\alpha(x) = -\alpha\cos(3x)\exp(-x^2/10) \leq -\alpha\frac{1}{2}\sqrt{2}\exp(-x^2/10) < -\alpha\frac{1}{2}\sqrt{2}\frac{1}{2}\sqrt{2} = -\alpha/2$$

if $x \in J$. □

Lemma 2. *If $x < -\alpha/2$ and $\alpha > \alpha_{p_1}$, where α_{p_1} is the larger root of the equation $\alpha^2 - 40\ln(3\alpha) = 0$, then $f_\alpha(x) \in \operatorname{int} J$. The value of α_{p_1} is approximately $\alpha_{p_1} \approx 11.968045$.*

Proof. Consider the inequality

$$\alpha\exp\left(-\frac{\alpha^2}{40}\right) < \frac{\pi}{12}.$$

By taking the logarithm on each side, and observing that $12/\pi > 3$ we find that

$$\frac{\alpha^2}{40} - \ln\alpha > -\ln\frac{\pi}{12} > \ln 3.$$

The function

$$g(\alpha) = \alpha\exp\left(-\frac{\alpha^2}{40}\right)$$

is monotone decreasing if $\alpha \geq 2\sqrt{5}$, so $g(\alpha) < \pi/12$ for all $\alpha > \alpha_{p_1}$ where α_{p_1} is the larger root of the equation $\alpha^2 - 40\ln(3\alpha) = 0$. Now

$$|f_\alpha(x)| = \alpha|\cos(3x)|\exp\left(-\frac{x^2}{10}\right) \leq \alpha\exp\left(-\frac{x^2}{10}\right) \leq \alpha\exp\left(-\frac{\alpha^2}{40}\right) < \frac{\pi}{12}$$

if $\alpha > \alpha_{p_1}$ and $x < -\alpha/2$. □

Lemma 3. *If $\alpha > \alpha_{p_1}$ then there is a primitive period-two point in* int J.

Proof. Let $K_\alpha = [-\alpha, -\alpha/2]$. By lemma 1 and lemma 2 we have the following sequence:

$$J \xrightarrow{f_\alpha} K_\alpha \xrightarrow{f_\alpha} \text{int } J$$

so

$$f_\alpha^2 : J \to \text{int } J.$$

Hence there is a $x_0 \in \text{int } J$ with $f_\alpha^2(x_0) = x_0$. Note that $\alpha_{p_1} > 2\sqrt{5} > \sqrt{5} > \pi/12$ so $J \cap K_\alpha = \varnothing$, and therefore $f_\alpha(x) \neq x$ for all $x \in J$. □

Lemma 4. *If $\alpha > \alpha_{p_2}$, where α_{p_2} is the larger root of the equation*

$$\alpha^2 - 40 \ln\left(\frac{46}{15}\alpha^2\left(3 + \frac{\alpha}{5}\right)\right) = 0,$$

then $\left|D\left(f_\alpha^2(x)\right)\right| < 1$ for all $x \in J$. The value of α_{p_2} is approximately given by $\alpha_{p_2} \approx 18.878546$.

Proof. Let $u = f_\alpha(x)$. By the chain rule we have

$$\begin{aligned}
\left|D\left(f_\alpha^2(x)\right)\right| &= |Df_\alpha(u)|\,|Df_\alpha(x)| \\
&= \alpha^2 \left|3\sin(3u) + \frac{u}{5}\cos(3u)\right| \exp\left(-\frac{u^2}{10}\right) \left|3\sin(3x) + \frac{x}{5}\cos(3x)\right| \exp\left(-\frac{x^2}{10}\right) \\
&\leq \frac{46}{5}\alpha^2 |x| \left(3 + \frac{|u|}{5}\right) \exp\left(-\frac{u^2}{10}\right) \\
&\leq \frac{46}{5}\alpha^2 \left(3 + \frac{\alpha}{5}\right) \exp\left(-\frac{\alpha^2}{40}\right) |x|.
\end{aligned}$$

Hence $\left|D\left(f_\alpha^2(x)\right)\right| < 1$ for all $x \in J$ if

$$\frac{\exp\left(\frac{\alpha^2}{40}\right)}{\frac{46}{5}\alpha^2\left(3 + \frac{\alpha}{5}\right)} > \frac{\pi}{12}.$$

Note that $1/3 > \pi/12$ so by rewriting the inequallity above we obtain the condition

$$\alpha^2 - 40 \ln\left(\frac{46}{15}\alpha^2\left(3 + \frac{\alpha}{5}\right)\right) > 0.$$

□

Lemma 3 and 4 imply that f_α has a period-two attractor for all $\alpha > \alpha_{p_2}$. Hence there exists an $\alpha_p \leq \alpha_{p_2}$ such that f_α has a period-two attractor for all $\alpha > \alpha_p$.

Let $A(f_\alpha)$ denote the domain of attraction of the period-two attractor. Its is clear by lemma 4 that $A(f_\alpha) \neq \varnothing$, and since $\mathbf{Fix}(f_\alpha) \neq \varnothing$ (by the intermediate value theorem) we see that $A(f_\alpha) \neq I_\alpha$. Let $K'_\alpha = I_\alpha \setminus [-\alpha, \alpha/2)$. We note that

$$A(f_\alpha) = \bigcup_{n \geq 0} \left(f_\alpha^{-n}(\text{int } J) \cap I_\alpha\right)$$

so if I_α is equipped with the relative topology we see by continuity of f_α that $A(f_\alpha)$ is open in I_α. Moreover is is easy to see that $A(f_\alpha) \supset K_\alpha \cup J \cup K'_\alpha$.

We remark that $I_\alpha \setminus A(f_\alpha)$ is an unstable chaotic Cantor set. We also remark that the upper bound for α_p is much larger than the actual value for α_p. The reason for this is the choice of the interval J made to simplify the calculations. As seen from the numerical experiments we have $\alpha_p \approx 6.85$.

5. Non-monotone families and antimonotone parametervalues

Let $\Lambda \subset \mathbb{R}$ be an interval, and let $\{f_\lambda\}_{\lambda\in\Lambda}$ be an one-parameter family of discrete dynamical systems on $\mathbb{R}$ or $\mathbb{R}^2$.

A bifurcation parameter value λ_0 is called orbit creating if new periodic orbits are created, and no periodic orbits are annihilated, at $\lambda = \lambda_0$. A bifurcation parameter value λ_0 is called orbit annihilating if periodic orbits are annihilated, and no new periodic orbits are created, at $\lambda = \lambda_0$. A bifurcation parameter value λ_0 is called neutral if no periodic orbits are annihilated and no periodic orbits are created at $\lambda = \lambda_0$ (transcritical bifurcations).

A family $\{f_\lambda\}_{\lambda\in\Lambda}$ is said to be monotone increasing if every bifurcation parameter value in Λ is neutral or orbit creating, and a family $\{f_\lambda\}_{\lambda\in\Lambda}$ is said to be monotone decreasing if every bifurcation parameter value is neutral or orbit annihilating. A family $\{f_\lambda\}_{\lambda\in\Lambda}$ is called non-monotone if Λ contains both orbit creating and orbit annihilating parameter values. A parameter value λ_0 is called anti-monotone if every neighborhood of λ_0 in Λ contains both orbit creating and orbit annihilating parameter values.

It is easy to construct a non-monotone family. Consider a cubic system of the form

$$f(x,\lambda) = x^3 + c_1x^2 + \lambda x + c_2.$$

c_1 and c_2 are coeffisients. Let $\mathcal{F}$ denote the set $f(x,\lambda) - x = 0$, and $\mathcal{D}$ the set $f_x(x,\lambda) + 1 = 0$ in the $x\lambda$-plane. Let $\mathcal{B} = \mathcal{F} \cap \mathcal{D}$. We see that λ_0 generically is a period doubling bifurcation parameter value if $(x_0,\lambda_0) \in \mathcal{B}$. Suppose (x_0,λ_0), $(x_1,\lambda_1) \in \mathcal{B}$ with $\lambda_0 < \lambda_1$ are two points in the same connected component of both $\mathcal{F}$ and $\mathcal{D}$ then the family $\{f_\lambda\}_{\lambda\in\Lambda}$, $\Lambda = [\lambda_0', \lambda_1']$ with $\lambda_0' < \lambda_0$ and $\lambda_1 < \lambda_1'$ is non-monotone. As an example

$$f(x,\lambda) = x^3 - \frac{83}{20}x^2 + \lambda x + \frac{1}{10}, \quad \lambda \in [3,5]$$

is non-monotone. Its bifurcation diagram is shown in figure 7. Here we see a stable fixed point bifurcating to a stable period two orbit and back to a stable fixed point as expected.

However, if we increase the distance between the points (x_0,λ_0), $(x_1,\lambda_1) \in \mathcal{B}$ we expect to see that also the stable period two orbit bifurcates to a stable period four orbit and back. This is shown in figure 8 with $f(x,\lambda) = x^3 - \frac{22}{5}x^2 + \lambda x + \frac{1}{10}$. By increasing the distance further we should expect to find infinite sequences of orbit creating parameter values, and infinite sequences of orbit annihilating parameter values. This is shown in figure 10 with

$$f(x,\lambda) = x^3 - \frac{9}{2}x^2 + \lambda x + \frac{1}{10}, \quad \lambda \in [2,6].$$

Let $\{f_\lambda\}_{\lambda\in\Lambda}$ be a C^3-family on $\mathbb{R}$ bifurcating from a simple periodic attractor to a chaotic invariant set containing a non-degenerate homoclinic orbit. We will now argue by heuristic arguments why existence of antimonotone parameter values should be a generic property of one-parameter families of the line. In [J] it is shown that a simple periodic attractor corresponds to a simple periodic attractor in the β-lift,

$$(x,y) \mapsto (f_\lambda(x) + \beta y, x),$$

and that a non-degenerate homoclinic orbit for f_λ corresponds to a transversal homoclinic point for the β-lift. Hence the β-lift has a chaotic invariant set containing a transversal homoclinic point. By fixing $\beta = \beta_0$ small, we see that the one-parameter family of diffeomorphisms of the plane

$$F_\lambda : (x,y) \mapsto (f_\lambda(x) + \beta_0 y, x)$$

bifurcates from a simple periodic attractor to a chaotic invariant set. Generically this will involve non-degenerate homoclinic tangency parameter values in the family F_λ, and by the antimonotonicity theorem in [K&K&Y] there will be antimonotone parameter values in the family F_λ. According to Newhouse [New]

there exist parameter intervals containing a dense set of parameters corresponding to non-degenerate homoclinic tangencies. By [J] the dynamics of the zero lift of f_λ is the same as the dynamics of f_λ, and the zero lift of f_λ is $|\beta_0| - C^r$-close to F_λ on compact sets, and hence there exist families containing antimonotone parameter values arbitrarly close to the zero lift. We expect these antimonotone parameter values generically to survive when going to the limit $\beta \to 0$, and only disappear when f_λ has special symmetries such as the logistic family. A sufficient condition for existence of antimonotone parameter values to survive the limit process is that the size of the Newhouse-intervals does not tend to zero generically when $\beta \to 0$. This viewpoint is supported by numercal evidence in figure 13 to figure 18. The bifurcation diagram does not change much when passing through $\beta = 0$.

6. The numerical experiments

The numerical experiments was performed on a Macintosh IIsi using the programs `ps-dyn` and `bif-tool` written by Tore M. Jonassen in Think C. The program `ps-dyn` produces PostScript output of phase-diagrams, bifurcation diagrams and Liapunov-exponent diagrams for discrete dynamical systems. The program `bif-tool` is a screen-zoom tool to investigate bifurcation diagrams.

In all figures the horizontal axis is the parameter axis, and the vertical axis is the phase space axis.

Figures 1 – 6 show both-ways pitch-forks for several different periodic orbits as predicted in section 3 with the family

$$f(x,\alpha) = -\alpha\cos(3x)\exp\left(-\frac{x^2}{10}\right).$$

Figure 1 shows the bifurcation diagram in the bi-modal parameter range. Let $r(\alpha)$ denote the right endpoint of the interval I_α. There is an $\alpha_{rf} \approx 1.075$ such that $f(r(\alpha),\alpha) < r(\alpha)$ if $\alpha < \alpha_{rf}$ and $f(r(\alpha),\alpha) > r(\alpha)$ if $\alpha > \alpha_{rf}$. At $\alpha = \alpha_{rf}$ we see that a stable fixed point comes into existence.

Figure 2 is a magnification of a part of left side of figure 1. We see periodic windows with both-ways pitch-forks as predicted in section 3. A window with a 10-periodic orbit with both-ways pitch-forks easily seen in the middle of the figure, and a window with a 11-periodic orbit with both-ways pitch-forks a little to the right.

Figure 3 is a magnification of the window with a 10-periodic orbit with both-ways pitch-forks from figure 2. The periodic points shown here is close to the right zero, z_2 of f_α. The structure of this figure seems to be similar to the both-ways pitch-fork sequences found in a cubic map (figure 10).

Figure 4 is a magnification of the window with a 11-periodic orbit with both-ways pitch-forks from figure 2. The periodic points shown here is close to the right zero, z_2 of f_α. Another infinite sequence of both-ways pitch-forks starting with a base period of 33 is also visible.

Figure 5 is a magnification of figure 2 near the upper right corner of the bifurcation diagram. Infinite sequences of both-ways pitch-forcs can be observed. They are however of a different type than the sequences in figure 3 and 4 as can be seen in figure 6.

Figure 6 shows a detail from figure 5.

Figures 7 – 12 contain the bifurcation diagram of the cubic systems constructed in section 5. Figures 11 and 12 are magnifications of the chaotic regions in figure 10.

Figure 7 shows a part of the bifurcation diagram for $f(x,\lambda) = x^3 - \frac{83}{20}x^2 + \lambda x + \frac{1}{10}$ in a non-monotone region. A stable fixed point bifurcates to a stable period-two orbit and back to a stable fixed point.

Figure 8 shows a part of the bifurcation diagram for $f(x,\lambda) = x^3 - \frac{22}{5}x^2 + \lambda x + \frac{1}{10}$. A stable period-four orbit comes into existence and disappears.

Figure 9 shows a part of the bifurcation diagram for $f(x,\lambda) = x^3 - \frac{14}{25}x^2 + \lambda x + \frac{1}{10}$. A stable period-sixteen orbit comes into existence and disappears.

Figure 10 shows a part of the bifurcation diagram for $f(x,\lambda) = x^3 - \frac{9}{2}x^2 + \lambda x + \frac{1}{10}$. We observe infinite sequences of both-ways pitch-forks and chaotic orbits. We believe there are intervals where the anti-monotone parameter values are dense.

Figure 11 contains a magnification of a region with both-ways pitch-forks and chaotic orbits.

Figure 12 is a magnification of the right part of figure 11. At this level only reversed pitch-forks are observed.

Figures 13 – 18 show the bifurcation diagram of singular perturbation of the β-lift of

$$f(x,\lambda) = x^3 - \frac{111}{25}x^2 + \lambda x + \frac{1}{10}$$

when passing from $\beta > 0$ small through $\beta = 0$ to $\beta < 0$ small. We have used $\beta = 0.05$, $\beta = 0.01$, $\beta = 0.005$, $\beta = 0$, $\beta = -0.0001$ and $\beta = -0.0005$. If we decrease β further, the bifurcation diagram looks like the bifurcation diagrams in figure 7 – 9.

Figures 19 – 24 show the bifurcation diagram of the family $f(x,\alpha) = -\alpha\cos(3x)\exp\left(-\frac{x^2}{10}\right)$ from section 2–4 with some details magnified. In particular we see that the family displays similar behavior as the cubic system in section 5 for parameter values slightly less than α_p, where the period two attractor comes into existence. We see in figure 24 that the period two attractor is born in a saddle-node bifurcation, as the previous period two attractor dies in a reversed saddle-node bifurcation. (The jump in the location of the period-two orbit.) Figures 21 – 23 show a part of the bifurcation diagram in the multi-modal parameter region.

References

[J] Tore M. Jonassen, *Singular perturbation of discrete systems*, Preprint, Dept. of Math., University of Oslo (1993).

[K] Ittai Kan, *Private communication* (1993).

[K&K&Y] Ittai Kan, Hüseyin Koçak and James A. Yorke, *Antimonotonicity: Concurrent creation and annilation of periodic orbits*, Annals of Mathematics **136** (1992), 219–252.

[New] Sheldon Newhouse, *The aboundance of wild hyperbolic sets and non-smooth stable sets for diffeomorphisms*, Publ. I.H.E.S. **50** (1979), 101–151.

[Pres] Chris Preston, *Iterates of Piecewise Monotone Mappings on an Interval*, Lecture Notes in Mathematics, 1347, Springer-Verlag, 1988.

Department of Mathematics, University of Oslo, P.O. Box 1053 Blindern, N-0316 Oslo
E-mail address: tojonass@math.uio.no

(x,y) = (0.000000,0.000000) ***Figure 1***
β = 0.000000 Map = 13, I = 200, P = 500
(α,x)∈ [1.024470,1.140480]×[−1.500000,1.500000]

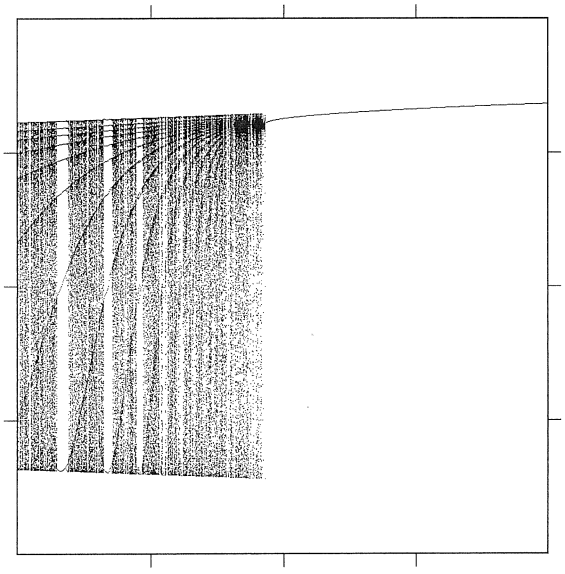

(x,y) = (0.000000,0.000000) ***Figure 2***
β = 0.000000 Map = 13, I = 200, P = 600
(α,x)∈ [1.040000,1.060000]×[−1.100000,1.100000]

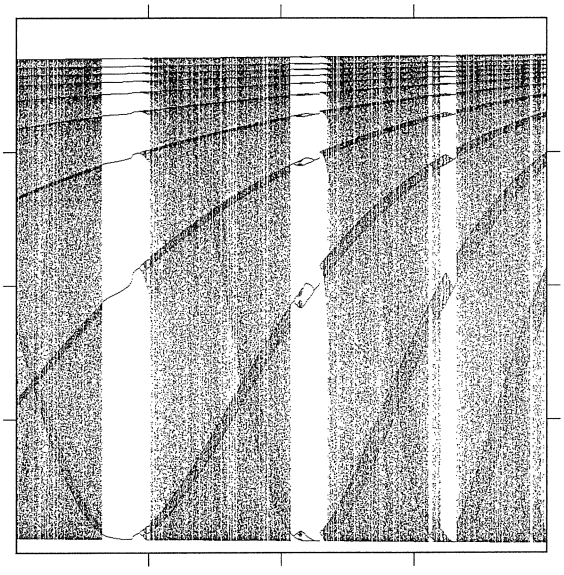

(x,y) = (0.000000,0.000000) ***Figure 3***
β = 0.000000 Map = 13, I = 300, P = 1000
(α,x)∈ [1.050417,1.051833]×[0.467500,0.595800]

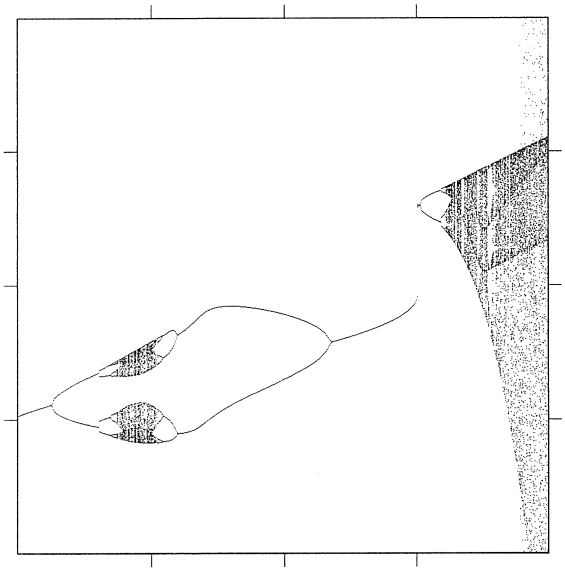

(x,y) = (0.000000,0.000000) ***Figure 4***
β = 0.000000 Map = 13, I = 300, P = 1200
(α,x)∈ [1.055000,1.056580]×[0.458000,0.577500]

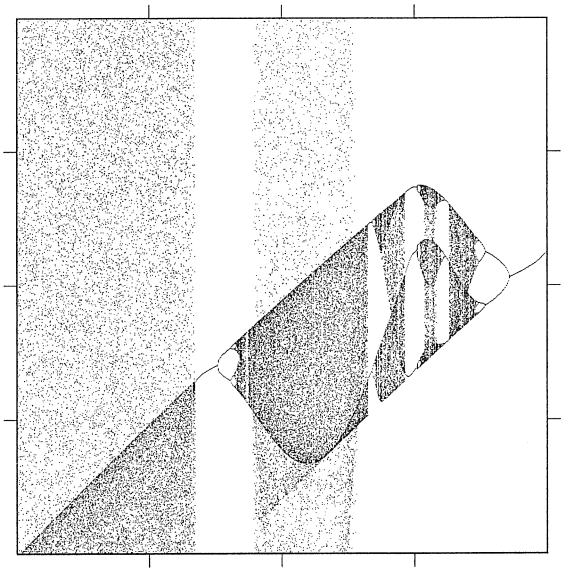

(x,y) = (0.000000,0.000000) ***Figure 5***
β = 0.000000 Map = 13, I = 300, P = 1200
(α,x)∈ [1.057920,1.060961]×[0.792100,0.969070]

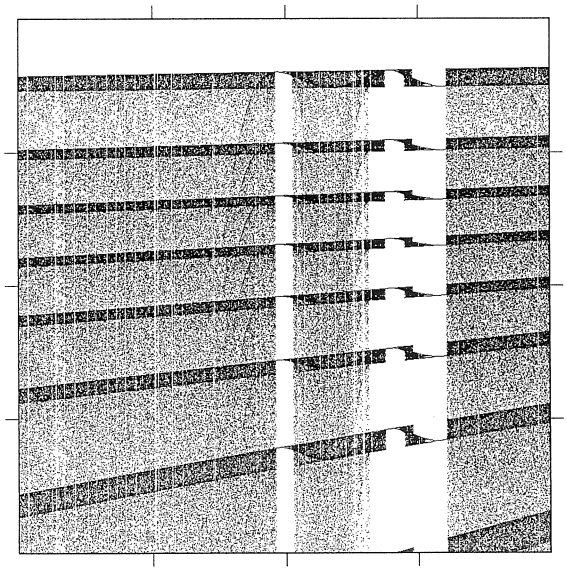

(x,y) = (0.000000,0.000000) ***Figure 6***
β = 0.000000 Map = 13, I = 300, P = 2000
(α,x)∈ [1.060026,1.060342]×[0.852594,0.864390]

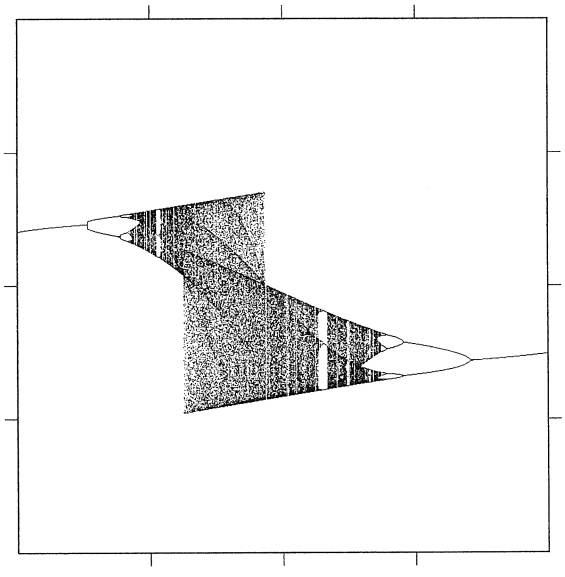

(x,y) = (0.200000,0.200000) ***Figure 7***
β = 0.000000 Map = 15, I = 50, P = 20
(α,x)∈ [3.000000,5.000000]×[0.000000,2.000000]

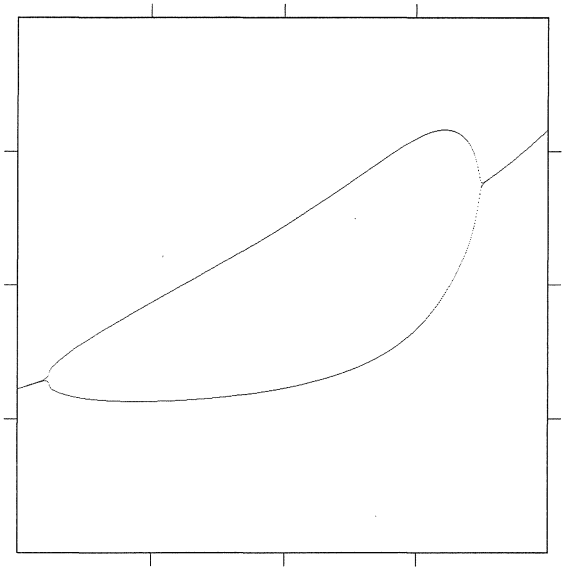

(x,y) = (0.200000,0.200000) ***Figure 8***
β = 0.000000 Map = 16, I = 50, P = 20
(α,x)∈ [2.000000,6.000000]×[0.000000,2.000000]

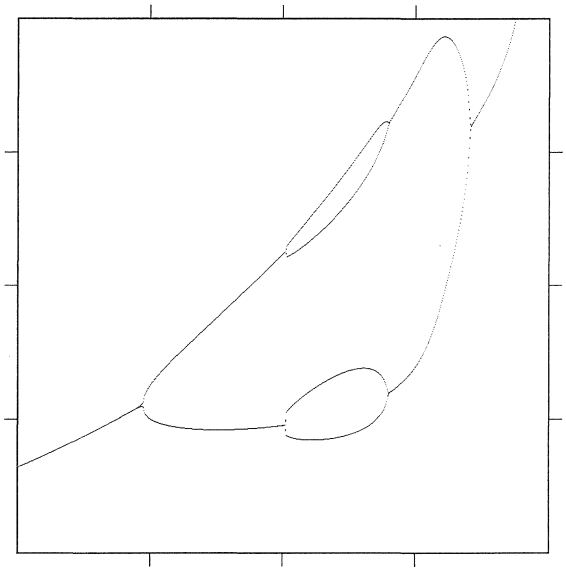

(x,y) = (0.200000,0.200000) ***Figure 9***
β = 0.000000 Map = 17, I = 50, P = 50
(α,x)∈ [2.000000,6.000000]×[0.000000,2.400000]

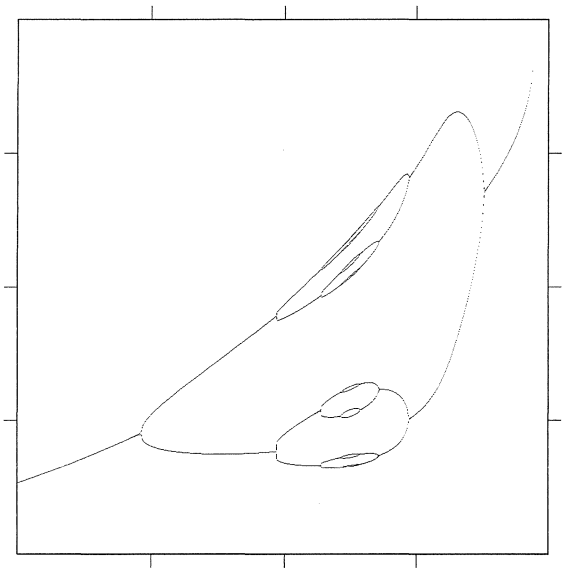

(x,y) = (0.200000,0.200000) ***Figure 10***
β = 0.000000 Map = 19, I = 50, P = 600
(α,x)∈ [2.000000,6.000000]×[0.000000,2.500000]

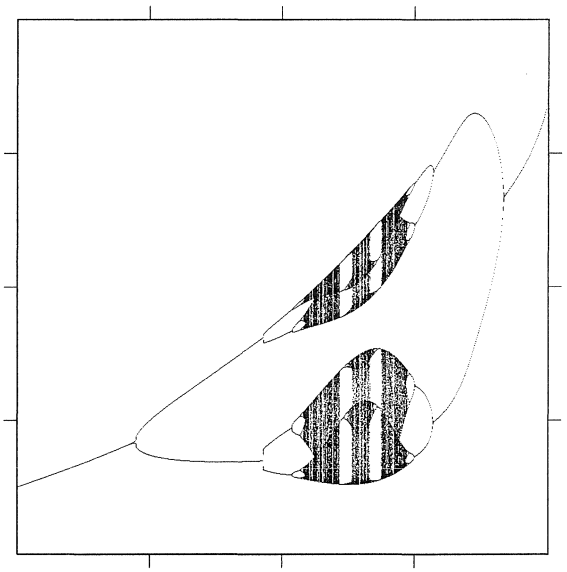

(x,y) = (0.200000,0.200000) ***Figure 11***
β = 0.000000 Map = 19, I = 50, P = 850
(α,x)∈ [4.466000,4.733000]×[1.000000,1.640000]

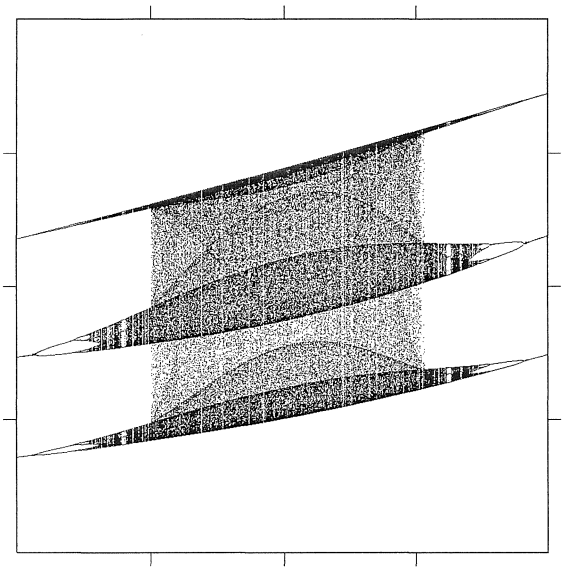

(x,y) = (0.200000,0.200000) ***Figure 12***
β = 0.000000 Map = 19, I = 50, P = 1100
(α,x)∈ [4.675150,4.729660]×[1.314670,1.394670]

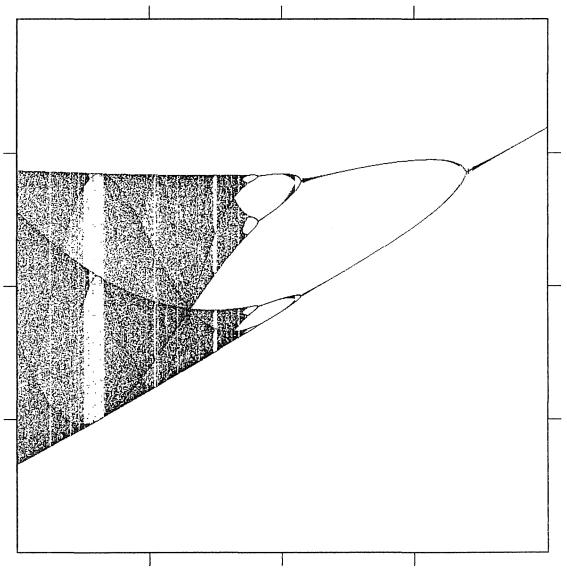

(x,y) = (0.200000,0.200000) ***Figure 13***
β = 0.050000 Map = 18, I = 100, P = 400
(α,x)∈ [2.000000,6.000000]×[0.000000,3.000000]

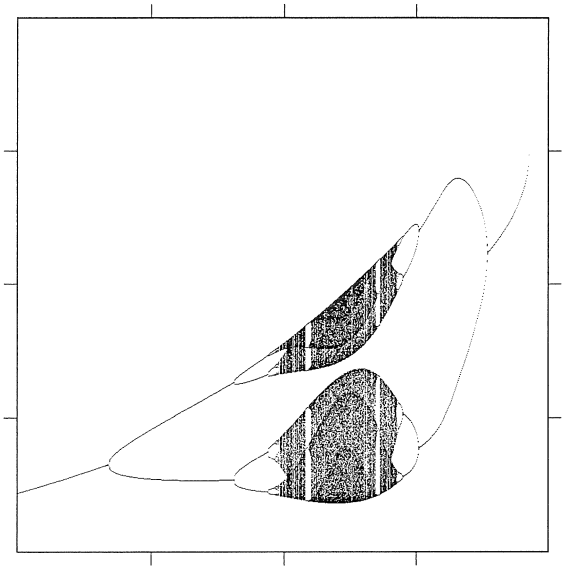

(x,y) = (0.200000,0.200000) ***Figure 14***
β = 0.010000 Map = 18, I = 100, P = 400
(α,x)∈ [2.000000,6.000000]×[0.000000,3.000000]

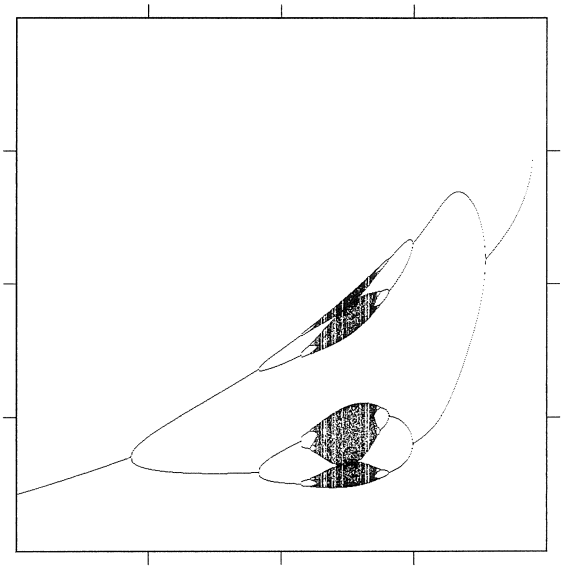

(x,y) = (0.200000,0.200000) ***Figure 15***
β = 0.005000 Map = 18, I = 100, P = 400
(α,x)∈ [2.000000,6.000000]×[0.000000,3.000000]

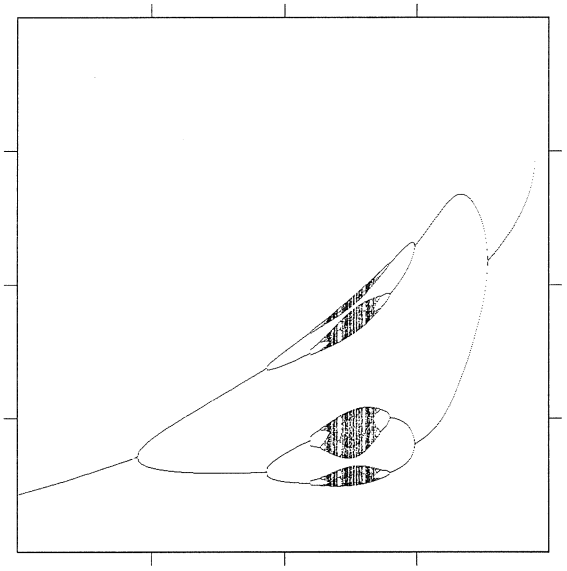

(x,y) = (0.200000,0.200000) ***Figure 16***
β = 0.000000 Map = 18, I = 100, P = 400
(α,x)∈ [2.000000,6.000000]×[0.000000,3.000000]

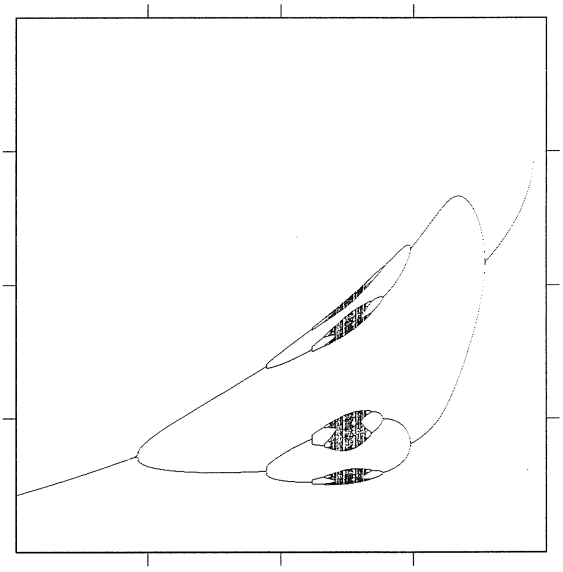

(x,y) = (0.200000,0.200000) ***Figure 17***
β = –0.000100 Map = 18, I = 100, P = 400
(α,x)∈ [2.000000,6.000000]×[0.000000,3.000000]

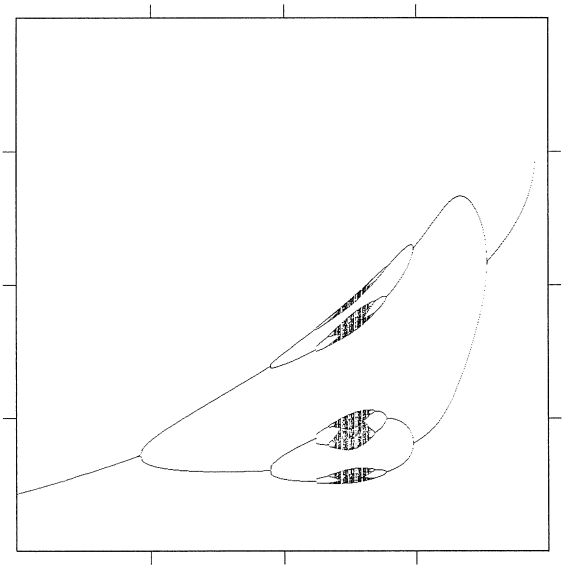

(x,y) = (0.200000,0.200000) ***Figure 18***
β = –0.000500 Map = 18, I = 100, P = 400
(α,x)∈ [2.000000,6.000000]×[0.000000,3.000000]

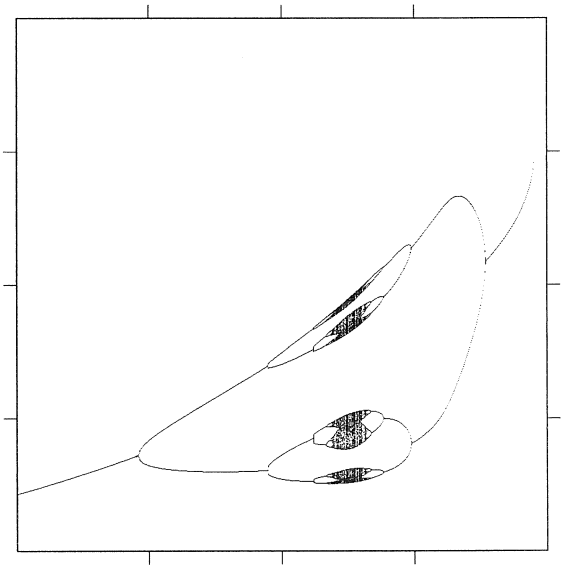

(x,y) = (0.200000,0.200000) **Figure 19**
β = 0.000000 Map = 13, I = 50, P = 200
(α,x)∈ [0.000000,10.000000]×[−10.000000,10.000000]

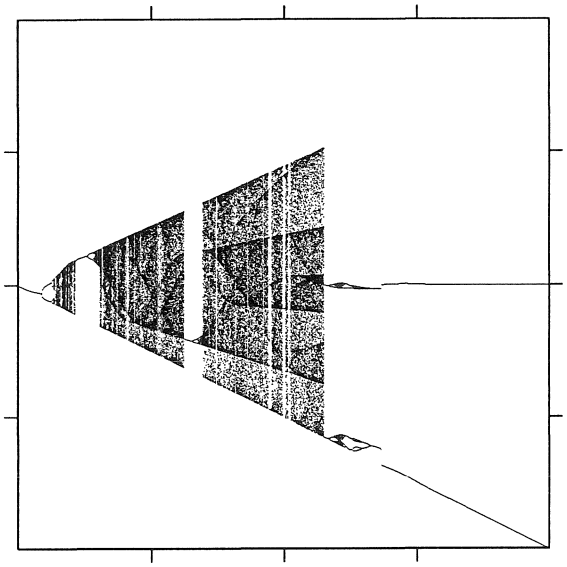

(x,y) = (0.200000,0.200000) **Figure 20**
β = 0.000000 Map = 13, I = 100, P = 400
(α,x)∈ [0.000000,1.083000]×[−1.100000,1.100000]

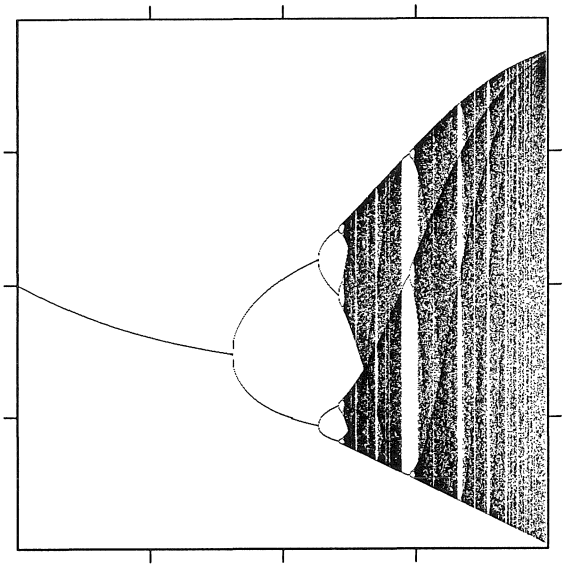

(x,y) = (0.200000,0.200000) **Figure 21**
β = 0.000000 Map = 13, I = 150, P = 800
(α,x)∈ [3.950000,4.125000]×[−4.250000,4.000000]

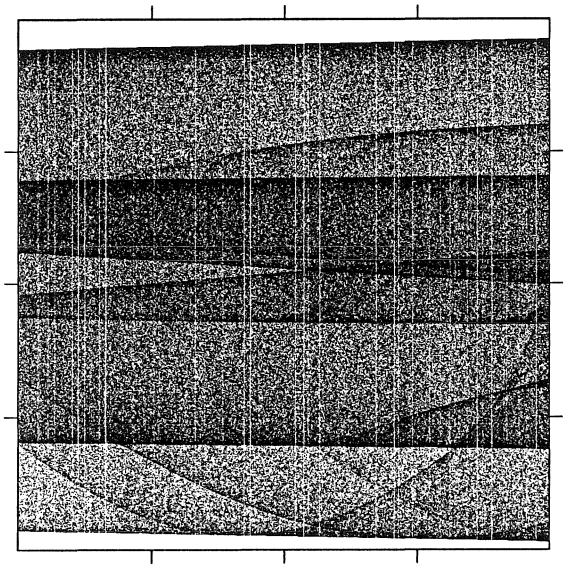

(x,y) = (0.200000,0.200000) **Figure 22**
β = 0.000000 Map = 13, I = 300, P = 1600
(α,x)∈ [4.081250,4.092361]×[−0.228125,0.425000]

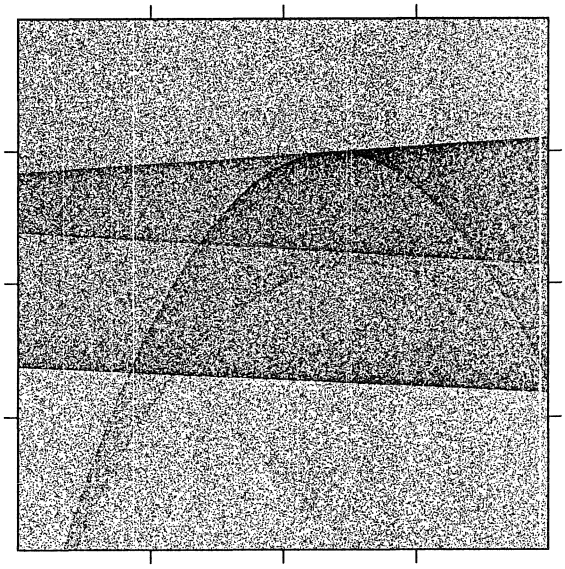

(x,y) = (0.200000,0.200000) **Figure 23**
β = 0.000000 Map = 13, I = 600, P = 3000
(α,x)∈ [4.088287,4.088472]×[0.253555,0.269883]

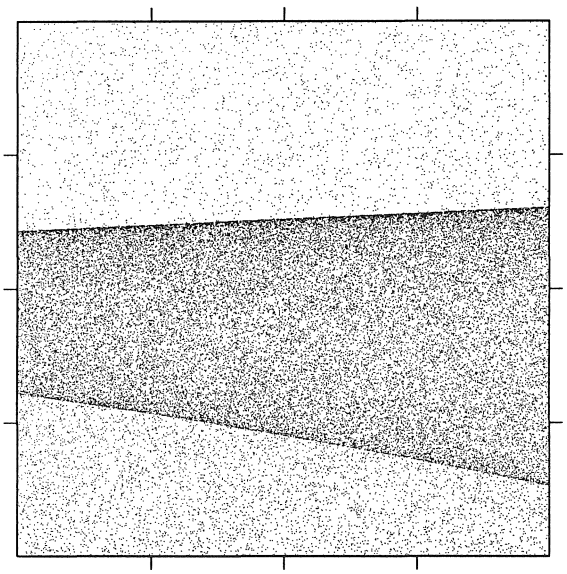

(x,y) = (0.200000,0.200000) **Figure 24**
β = 0.000000 Map = 13, I = 100, P = 600
(α,x)∈ [5.750000,7.300000]×[−0.250000,0.250000]